JOURNAL OF MATERIALS SCIENCE 6 (1971) 1465–1478

Cold Rolling of Polyethylene

Part 1 *The Superstructure of Cold Rolled Low Density Polyethylene as noted by XYZ Light Scattering*

GARTH L. WILKES
Department of Chemical Engineering, School of Engineering and Applied Science, Princeton University, Princeton, New Jersey 08540, USA

The morphology of unidirectional cold rolled polyethylene was investigated. The techniques of scanning electronmicroscopy, wide angle X-ray diffraction, DTA, and XYZ photographic light scattering were employed. Most of the study was undertaken using low density polyethylene which had been initially cold rolled to an elongation of 100% and then annealed under vacuum for 30 min at 92°C. Some work utilised rolled but not annealed material. The investigation illustrated that the use of the new technique of XYZ photographic light scattering was indeed successful in its application to the study of the morphology of such material. Use of this technique is suggested for similar studies on biaxially oriented films. It was also found that Keller's three zone material could be produced. Speculation is made about the morphology and texture of both the rolled and annealed and the rolled and unannealed material.

1. Introduction

In a previous series of papers by Keller *et al* [1-4], the morphology of drawn and subsequently rolled low density polyethylene has been discussed. The last of these papers [4] deals with the morphology resulting from unidirectional rolling without predrawing. We would like to add further support to the basic conclusions put forth by Keller *et al*, and report the use of photographic light scattering as an additional tool for investigating the complex morphological texture and superstructure that exists in such rolled films. At the same time, we would like to show that the photographic light scattering technique can be utilised to a greater extent that it has been by past workers [5-7]. Furthermore, it is anticipated that this initial paper will aid in the elucidation of the changes in superstructure that result from unidirectional rolling. Certainly such information is useful since many processing techniques involve the use of cold rolling. A much more comprehensive report is in preparation on the correlation between the orientation behaviour and morphology induced by cold rolling in both high and low density polyethylene.

2. Experimental

2.1. Preparation of Samples

An experimental low density (0.917) Phillips polyethylene sample of melt index 3.80 was used as the material. The weight average molecular weight was given to be 500000. A thick film (10 × 10 × 0.5 cm) was prepared by compression moulding between two flat platens at 160°C. Upon removal from the press the material was quenched in tap water. Strips about 1 cm wide were cut from the slab, and then cold rolled at 22°C in one pass to an elongation of about 100%. The roller apparatus will be described in more detail elsewhere. The thickness after rolling was reduced to 0.2 cm; the material was then annealed in a vacuum oven at 92°C for 30 min.

2.2. Wide Angle X-ray Diffraction

From the annealed sample thin sections were cut in the XY, YZ, and XZ planes – see fig. 1. To confirm the presence of Keller's "three zone" material, wide angle X-ray diffraction experiments were run near the outer edges (rolled surfaces) and in the core of a section cut in the

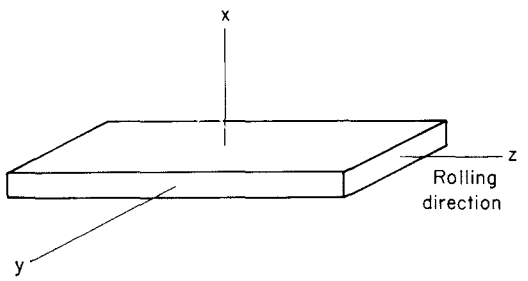

Figure 1 Drawing showing how the axes of the rolled film are designated.

XZ plane. The X-ray radiation was from a copper target and was passed through a nickel filter.

2.3. Low Angle Photographic Light Scattering (LS)

The LS technique was first introduced by Stein *et al* [5] and has been utilised by many others [6-8] in studying the superstructure of thin polymer films. The technique consists of passing a beam of polarised light through a sample as schematically illustrated by fig. 2. The scattered

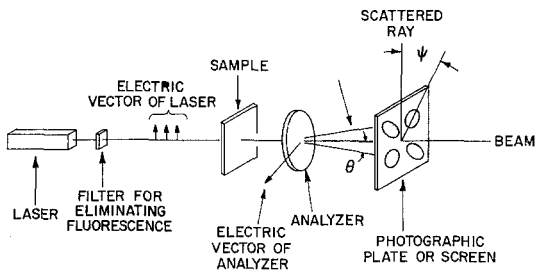

Figure 2 Schematic illustrating the typical photographic light scattering apparatus. Note the definitions of the scattering angles θ and ψ.

rays then pass through a second polariser generally termed the analyser. A photographic screen or an open front Polaroid camera placed a few inches behind the analyser records the LS pattern – see fig. 2. In the past, all investigations reported, at least to the author's awareness, have been made by passing the beam normal to only one plane in the film – specifically normal to the YZ plane. This type of LS will be denoted as *x*-axis LS in this paper. Such *x*-axis LS is suitable if the existing morphology is independent of the thickness, i.e. there are no skin effects, and secondly if biaxial orientation is not involved such as occurs during rolling, direct biaxial stretching, or even possibly as a result of annealing a deformed film. In biaxial orientation, to more fully understand the structure and superstructure, more than one plane or axis of the sample must be investigated, e.g. by use of pole figure X-ray diffraction or sectioning in different planes when microscopy techniques are applied. We propose here that the use of the LS technique should similarly be used and will demonstrate that in doing so substantially more information can be gained which can lead to a better and more realistic interpretation of the superstructure. To do this, one simply sections the sample film into various planes such as those of XY, XZ, and YZ etc., see fig. 1. For best results one prefers thin transparent sections (a few mm thick) with as smooth a surface as possible. The smooth surface helps to minimise surface scattering which is further eliminated by use of an immersion oil of matching refractive index to that of the sample. The sections are then investigated by use of the LS technique in the conventional way. Generally, since the smaller dimension of the plane normal to the beam is less than the diameter of the beam of a laser, pinhole collimation must be used to decrease the beam to a diameter less than this sample dimension. This in turn generally necessitates longer exposure times for recording the LS pattern.

In *x*-axis LS patterns there is some common notation used for denoting the orientation of the electric vectors of the polariser, P, and analyser, A, relative to each other as well as to the stretch axis. Specifically, V_V denotes that the analyser, V, is aligned parallel with the stretch direction and also the polariser, v. H_h is similar except both analyser, H, and polariser, h, are now perpendicular to the stretch axis. Similarly, H_V means that the analyser, H, is perpendicular to both the polariser, v, and to the stretch axis. Such notation is difficult to use throughout this paper since in some cases the beam is propagating along the stretch or rolling axis, Z. Hence in the LS patterns from the *rolled* material we will simply refer to a parallel pattern, PP, as a pattern where the electric vectors of both polariser and analyser are parallel and a crossed polar pattern, CP, as one where these two vectors are perpendicular to each other. At the same time, however, we will show simultaneously, with each pattern, just how the axes of the sample section were aligned with respect to these vectors. If one so desired, a notation system

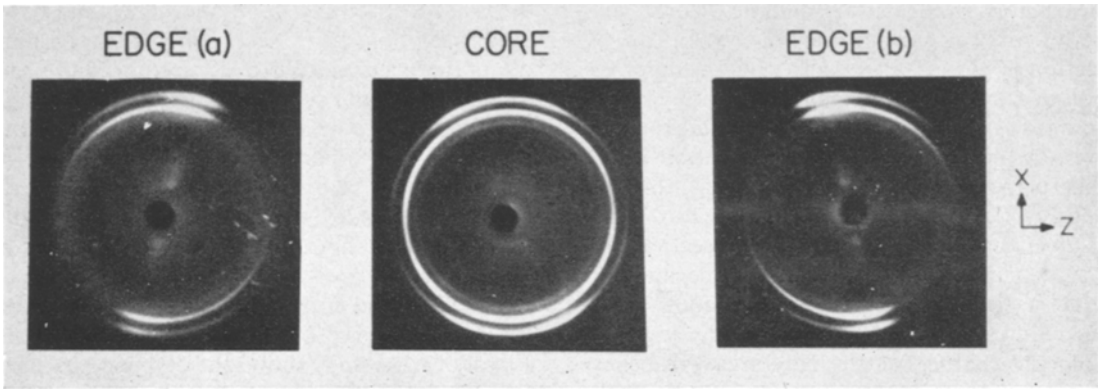

Figure 3 Wide angle X-ray diffraction patterns from the rolled and annealed film taken with the X-ray beam along Y.

using additional subscripts on the H, V, h, or v designation could be used in such work, e.g., H_yv_x might refer to the analyser lying along Y, the polariser along X, and thus Z must therefore be the beam axis.

3. Results

3.1. X-ray Diffraction

Fig. 3 shows the results of the experiments when the X-ray beam was passed down the *y*-axis. It should be clear that at the edges a nearly single unit cell texture is present yet one edge shows an opposing texture (mirror image) to that of the other edge. The core, on the other hand, clearly appears to be a superposition of the textures existing at the edges. These are in good agreement with Keller's three zone material. The wide angle X-ray pictures taken of a section with the beam in the Z direction are shown in fig. 4. Although there is some difference in intensity, the pattern taken at the edge is essentially identical to that of the core. It seems apparent, however, that a more prominent "six point" (1 1 0) and (2 0 0) reflection is present in the core pattern. This is indicative of twinning as has been discussed by Keller [4]. The aspect of, or nature of, such twinning will not be discussed further in this paper. Wide angle pictures taken through a YZ section with the beam along X also show essentially identical orientation where there is strong (0 2 0) and (1 1 0) equatorial diffraction.

3.2. Microscopy

Although not illustrated in this paper, it was

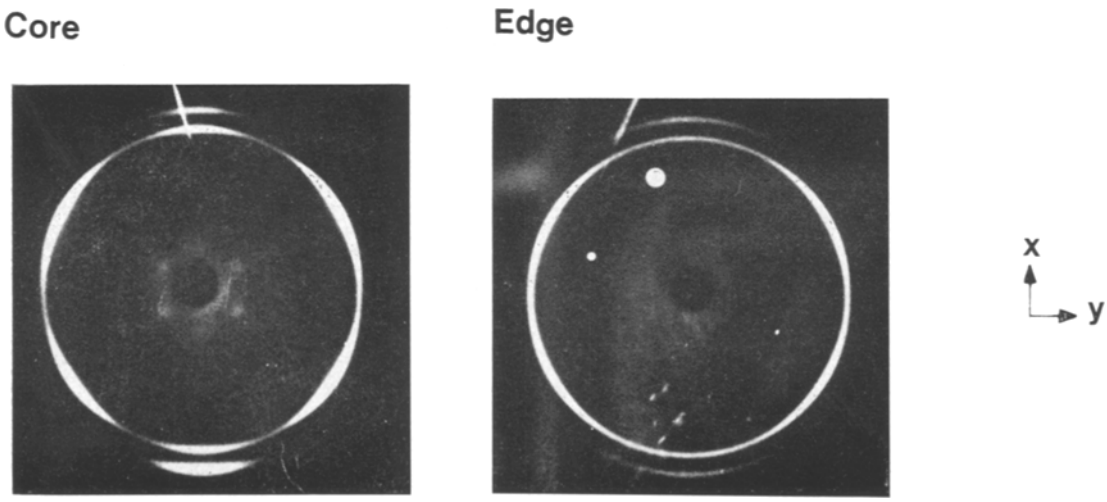

Figure 4 Core and edge wide angle X-ray diffraction patterns from the rolled and annealed film with the X-ray beam along Z.

clearly observed that a definite "core" exists between two surface regions when an XY section is viewed in a microscope using crossed polarisers. In our sample the core structure composed about 60% of the total thickness. We are now making a further investigation on how this percentage depends on initial thickness, degree of rolling, annealing temperature, etc.

Electron micrographs of an XY section taken with a scanning electron microscope illustrated that a much more inhomogeneous texture existed in the core area relative to the edges. The "blocky" nature of the core area was believed to be due to remnants of, or intact, spherulitic crystalline regions. These observations would seem consistent with the X-ray diffraction results since they support a single crystal axis orientation at the edge which would not be so apparent if the true spherulitic character were preserved. Further support of this speculation will also be given shortly by use of XYZ light scattering technique which has been described earlier in the paper.

3.3. XYZ Light Scattering

Fig. 5 shows the typical spherulitic x-axis light scattering patterns that generally occur from an undeformed polyethylene sample. Drawn samples of this same material give similar patterns except that the H_V "four leaf clover" pattern deforms in a predictable fashion [5, 6]. The H_h pattern (not shown) generally bears some similarity to the V_V but is rotated 90 degrees. Figs. 6*a-c* show the x-axis CP patterns for the edges and core material (obtained by sectioning the initial film, along the x-axis, into five YZ sections and using sections 1, 3 and 5 for x-axis light scattering). Patterns a-c are quite similar to each other, but there are subtle differences in these patterns which will not be discussed in the present work. The PP patterns are represented by d and e. Both core and edge shots gave similar PP patterns as labelled. Figs. 7*a-h* show various patterns taken in the edges and core of an XY section, i.e. with the laser beam propagating along the x-axis. Finally, figs. 8*a-i* show the typical patterns taken with the beam propagating along the y-axis, i.e. normal to an XZ section.

4. Discussion

From the LS photographs it should be clearly apparent that the technique of XYZ light scattering gives distinct clear patterns and likely offers further information on which to propose a morphological model. The technique should, therefore, be considered as a potential aid in morphological studies, when applicable, *especially* where other than uniaxial deformation is involved. In fact, it is quite surprising that y and z-axis light scattering has not been used before in conjunction with x-axis light scattering. Such XYZ light scattering clearly has the ability to illustrate the effects of biaxial orientation. It should be noted that the technique of XYZ light scattering has also been successfully applied by this author to uniaxial deformed polyethylene [9].

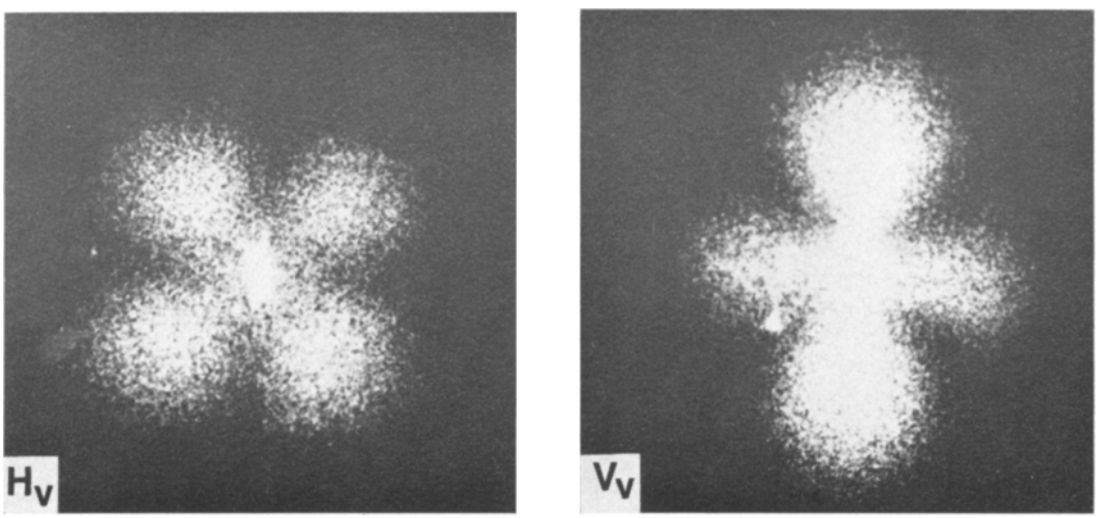

Figure 5 Typical H_V and V_V light scattering patterns from an undeformed polyolefin such as polyethylene. (*a*) H_V, (*b*) V_V.

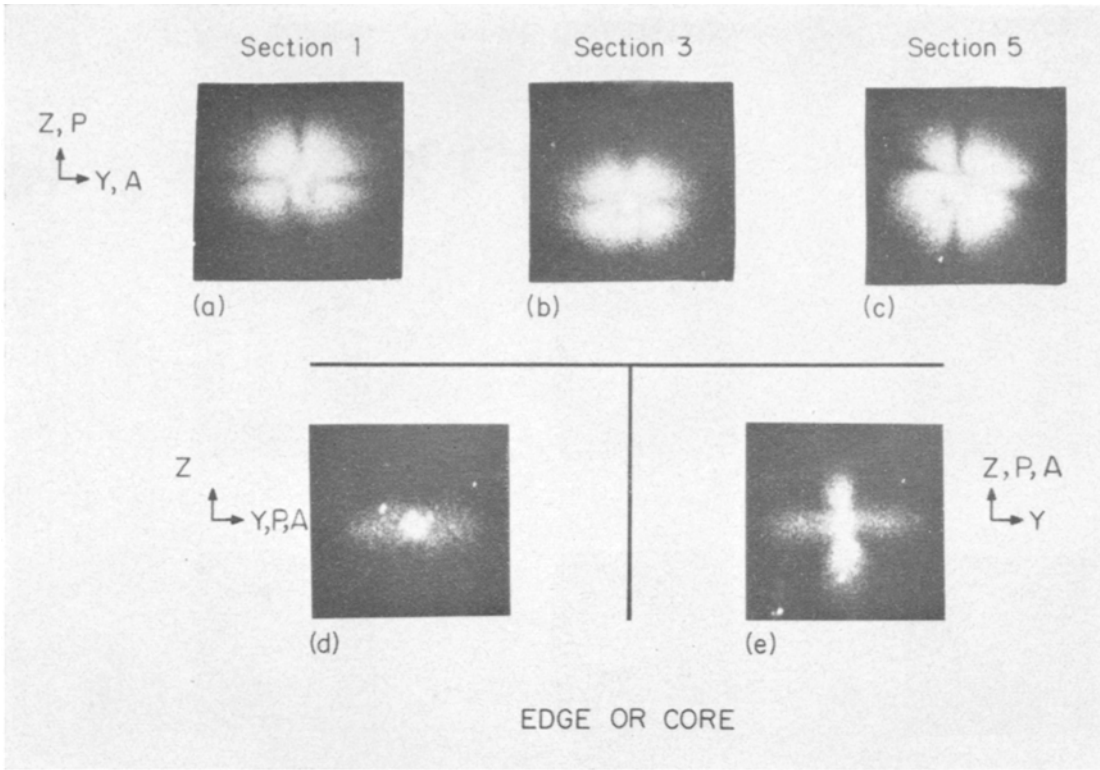

Figure 6 *x*-axis LS patterns taken in the rolled and annealed film which has been first sectioned perpendicular to the *x*-axis. The PP patterns are equivalent whether taken in the core or the edge.

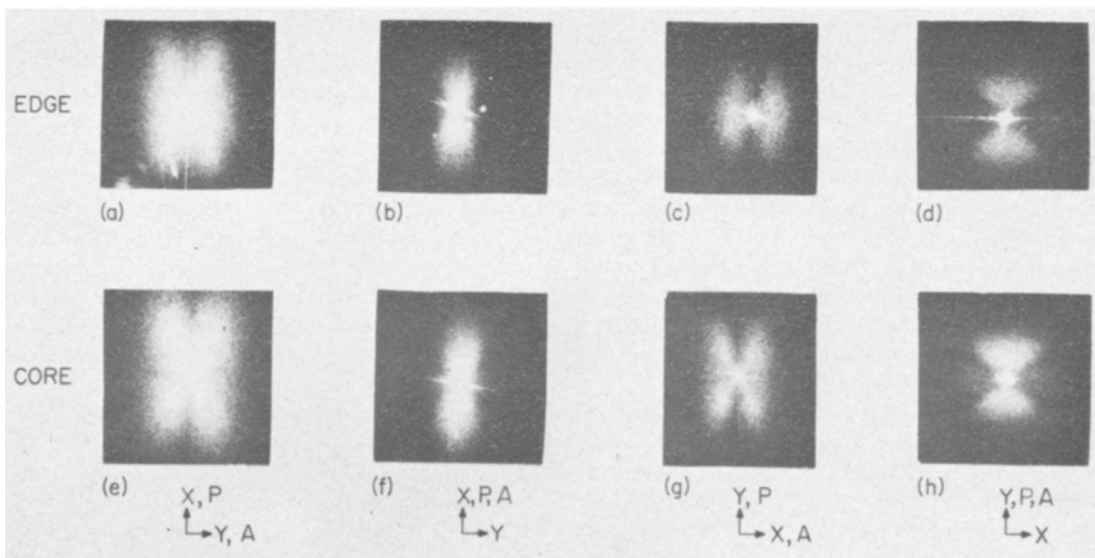

Figure 7 *z*-axis LS pattern taken in the rolled and annealed film. Both core and edge patterns are shown as labelled.

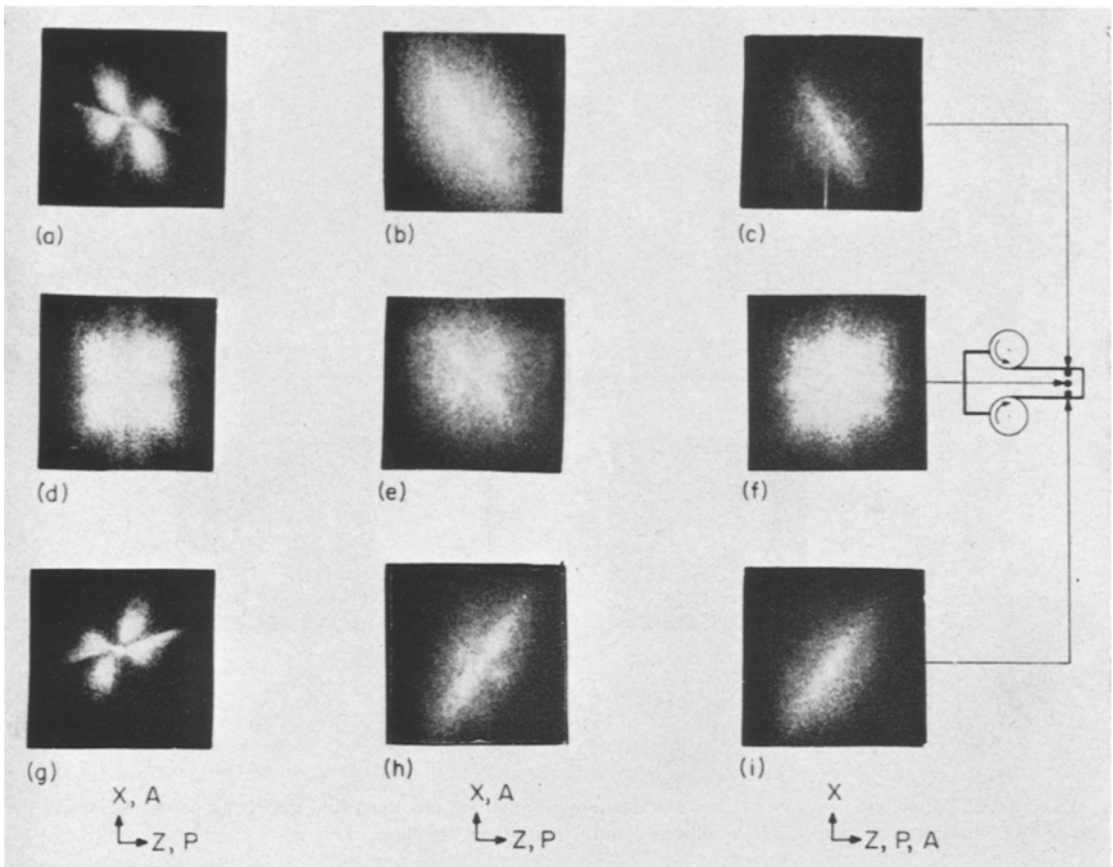

Figure 8 *y*-axis LS patterns taken in the rolled and annealed film. An indication of the location where the beam entered the sample is illustrated by the arrows at the right. The revolving circles at the right represent an end view of the rollers.

We must now question whether or not our light scattering results support Keller's earlier proposal regarding the single texture of the edges and the double texture character of the core on the unidirectionally rolled and annealed polyethylene. It should be partially apparent from comparison of fig. 8 with the wide angle X-ray pictures (fig. 3) that there is some definite correlation with respect to symmetry of the patterns. Indeed there is also correlation between the *z*-axis wide angle X-ray diffraction and *z*-axis LS patterns. Specifically, in the case of the *z* pictures it is clear that for all general purposes, the patterns from X-ray or from light scattering are very similar whether taken in the core or at the edge. This was also true for the *x*-axis X-ray diffraction pictures (not shown) and LS patterns. This clearly is not true for the *y*-axis pictures where differences in each edge are apparent yet the pattern from the core appears to be somewhat a superposition of the two edge patterns.

Sufficient theoretical light scattering calculations have not as yet been made to warrant quantitative explanation of the data generated by the application of XYZ light scattering. However, qualitative or speculative explanation is in order since many of the patterns can be related to the familiar *x*-axis spherulitic scattering patterns already theoretically explained [5].

First of all, the *x*-axis CP and PP patterns (figs. 6*a-e*) indicate deviation from the typical spherulitic patterns as was shown in figs. 5*a-b*. Clearly there is a "four leaf clover" nature to the CP patterns, but the lobes are no longer well rounded. The most "spherulitic-like" pattern is that taken in the core (fig. 6b) but this too is not "typical" of a uniaxially deformed spherulite. It also does not fit the theoretical H_v (crossed polar)

patterns for disk spherulites as calculated earlier by Clough *et al* [10]. Realistically, however, one might not think that a disk model would be useful in this case since the mode of deformation is not to deform a sphere into a disk but rather into something that might resemble, as a first approximation, a partially flattened football as shown by fig. 9. The *x*-axis PP patterns (V_v and H_h) (figs. 6*d* and *e*) are also only in general agreement with those expected from a spherulitic texture – compare with the V_v pattern of fig. 5.

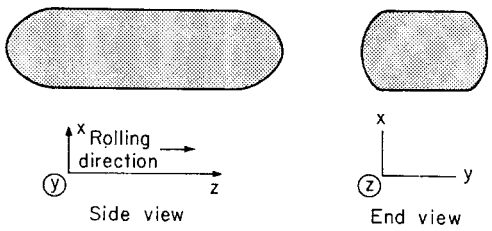

Figure 9 Schematic of "flattened football" model used as a first approximation in explaining the core structure.

The flattened football model is useful but is certainly not totally correct in light of the *z*-axis wide angle X-ray pictures. It certainly does not seem logical to be a correct model for the edges since it is difficult to correlate this model with a single crystalline texture as the X-ray patterns suggest. It is for these latter reasons that the *x*-axis patterns, particularly those from the edge section, are believed to arise not only from spherulite origin (or remnants of spherulites) but may also originate from imposed internal strains occurring in the deformed amorphous regions and/or pulled apart spherulites to form the single crystalline texture. The theory of strain scattering has been given elsewhere [11].

With regard to the LS patterns with the beam in the Z direction, fig. 7, one sees little or no difference between those taken in the edge and those taken in the core. This implies that the beam encounters a similar anisotropic environment in either location. We note that the wide angle X-ray pictures taken with the beam along Z also give similar results in the core as at the edge (figs. 7*a* and *b*). We do see, however, that these LS patterns (figs. 7a-*h*) somewhat resemble scattering from deformed spherulites. Specifically, the CP pictures show deformed lobes yet these photos also indicate that there is no distinct maximum in intensity as a function of scattering angle θ (refer to fig. 2) as is noted in typical spherulitic scattering. The PP patterns of fig. 7 similarly give patterns that somewhat resemble V_v or H_h type patterns of spherulitic structure yet, on closer inspection, there are some definite differences when compared with fig. 5. Such differences are not totally unexpected here since biaxial orientation is present and hence the local anisotropy is different from that which exists following uniaxial deformation.

LS patterns taken with the beam along the *y*-axis are shown in figs. 8*a-i*. Two CP series are shown in these figures since these were found in the same sample. The series of figs. 8*a*, *d*, and *g* is the most typical of the patterns found however and will be those which are qualitatively discussed at this point. The PP patterns were essentially the same for either series. Here each edge gives a different pattern and the pattern of one edge is the mirror image of the other. The pattern of the core is also somewhat equivalent to the superposition of the two edge patterns. This observation is most clear in the CP patterns, but it also holds for the PP patterns as well. This type of superposition of edge patterns was also found by Keller in the small angle pole figures for the long spacing as well as for the pole figures for the (1 1 0) planes (*c*-axis orientation) and 2 0 0 planes (*a* axis orientation).

The wide angle X-ray technique gives information on crystalline unit cell orientation, the small angle X-ray technique gives information on the average long spacing or the average crystalline lamellar-amorphous period. Light scattering, on the other hand, has the ability to detect alterations of the superstructure that may occur over distances on the order of microns where either of the other two techniques cannot be easily utilised e.g. one can determine average spherulite size by the light scattering method but not by the other two methods [5]. Having information from all these three methods* we are now in a position to propose a simple model, at least to a first approximation, of the superstructure in the *core* of this material. It should be made clear at this point that what follows is over-simplified and is not offered as an explanation for more highly rolled low density polyethylene or high density polyethylene. Such investigations which have been undertaken will be published at a later time. Fig. 10 presents a sketched summary of the light scattering patterns; below these is sketched

*We are reasonably assuming that if small angle patterns were available they would be equivalent to those given by Keller [4].

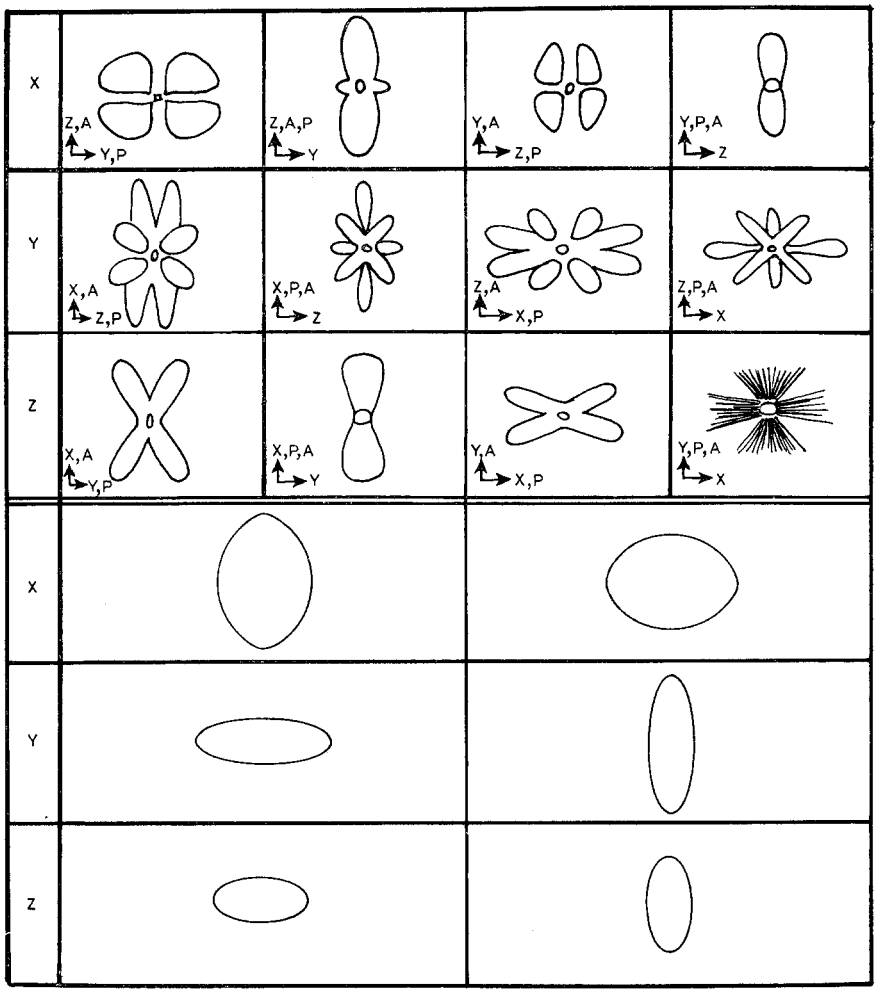

Figure 10 Sketched summary of X, Y, and Z LS patterns taken from the core of the rolled film. Below these patterns is shown how the "flattened football" model should appear to the incoming incident beam.

how the incoming beam might see the elongated and flattened spherulite (flattened football) which will now be used to help rationalise the superstructure and yet try to maintain consistency within the framework of the wide and small angle X-ray data†. As stated above, this discussion will be first directed at the superstructure of the core material and thus fig. 10 should not be considered to represent the model of the edge material which will be discussed later. Also given as an aid in this discussion are equations 1 and 2, which are the familiar theoretical equations describing the H_V and V_V scattering intensity from spherulitic structures [5]. These equations are

$$I_{Vv} = AV_0^2\left(\frac{3}{U^3}\right)^2\Big[(\alpha_t - \alpha_s)(2\,\mathrm{Sin}U - U\mathrm{cos}U - \mathrm{Si}U) + (\alpha_r - \alpha_s)(\mathrm{Si}U - \mathrm{Sin}U) - (\alpha_t - \alpha_r)\,\mathrm{Cos}^2\left(\frac{\theta}{2}\right)\cdot\mathrm{Cos}^2\psi\,(4\,\mathrm{Sin}U - U\mathrm{Cos}U - 3\mathrm{Si}U)\Big]^2$$

$$I_{Hv} = AV_0^2\left(\frac{3}{U^3}\right)^2\Big[(\alpha_t - \alpha_r)\,\mathrm{Cos}^2\left(\frac{\theta}{2}\right)\mathrm{Sin}\psi\mathrm{Cos}\psi\,(4\mathrm{Sin}U - U\mathrm{Cos}U - 3\mathrm{Si}U)\Big] \qquad (2)$$

†The author is again referring to the small angle X-ray pole figures of Keller.

where V is the volume of the spherulite, α_t and α_r are the tangential and radial polarizabilities of the spherulite, α_s is the surrounding polarizability while θ and ψ are the radial and azimuthal scattering angles (see fig. 2), A is a proportionality constant, and SiU is a sine integral defined as

$$\mathrm{Si}U = \int_0^U \frac{\mathrm{Sin}\, X}{X}\, \mathrm{d}X \tag{3}$$

the term U is defined as

$$U = (4\, Ro/\lambda')\, \mathrm{Sin}\, (\theta/2) \tag{4}$$

where Ro is the radius of the initially undeformed spherulite and λ' is the wavelength of the beam in the sample. With equations 1 and 2 patterns similar to those in fig. 5 can be predicted. By adding a shape dependence of the scattering body to the term U, it has been shown that x-axis type H_v and V_v patterns can be predicted for uniaxially deformed polyethylene [6] or polypropylene [8]. As expected, such patterns, although not shown here, do not completely explain the types of patterns that appear in the rolled films. As already discussed, however, the fact that the four lobe CP patterns and the PP patterns also somewhat resemble the predicted patterns following uniaxial deformation gives assurance that one is still maintaining some spherulitic texture in the rolled and annealed films. The local morphology, on the other hand, is expected to be more complex after rolling than is the case in uniaxially drawn material–this is clear from the wide angle X-ray data alone.

We, as yet, have not attempted to generate new models from which to calculate theoretical patterns to compare our experimental results against. It is speculated, however, that just introducing a shape dependence in the U term of equations 1 and 2 will not suffice for biaxial deformations such as occur in cold rolling. It would also seem reasonable in biaxial deformation that due to the generation of a nonhomogeneous internal strain field, the terms $(\alpha_t - \alpha_s)$, $(\alpha_r - \alpha_s)$ and $(\alpha_t - \alpha_r)$ should be a function of the scattering angles θ and ψ – particularly as the degree of deformation increases.

Inspecting the patterns more closely with the beam along the z-axis (figs. 10i, j, k and l), we see that in the CP patterns (i and k) there exists a deformed "clover leaf" type pattern representative of a deformed spherulite where the long axis of the spherulite is perpendicular to the long axis of the pattern (i.e. perpendicular to the bisector of the smaller of the two angles between the lobes). From past theory [10] the patterns are in agreement with the simple model proposed as shown in the same figure. These patterns, however, do not seem to possess a distinct maximum in intensity as a function of the scattering angle θ. We do not wish to discredit the deformed spherulite explanation, but, as mentioned earlier, to suggest this lack of a distinct maximum may be due to scattering caused by nonspherical, internal strain fields surrounding spherulitic regions or separate spherulites. This type of scattering superimposed on the deformed spherulite scattering could lead to a lack of a distinct maximum in intensity as a function of θ. An alternative explanation is that the rolling process may induce spherulitic disorder which is angularly dependent, that is, the degree of disorder or change in local spherulitic anisotropy may depend on the angle the fibrillar axis of a spherulite initially makes with the rolling direction. The result of such deformation can also lead to a lack of a distinct maximum in the scattered intensity when measured as a function of θ.

Further support for the presence of spherulitic structure in the core follows from inspection of the PP patterns of fig. 10. Although these patterns are certainly not completely comparable with that obtained from a deformed three-dimensional spherulite. they do in fact give some agreement with those expected. It should be recalled that the intensity of the PP patterns depends not only on the anisotropy, i.e. $\alpha_t - \alpha_r$, but upon terms involving the local polarizability of the surroundings, α_s – see equation 1. The result of this is that the PP patterns are much more sensitive to local morphological changes than the crossed polar (CP) arrangement. Also we believe that since biaxial orientation is present, the local environment, and polarizability at one point relative to another, depend on the vector connecting any two points and not just the distance. This results in a complexity in morphology that is shown by the fact that the resulting LS patterns depend on the propagation axis of the incident beam, i.e. x, y, or z. A further point of complication is that no theoretical work is available as yet that describes how the PP patterns depend on internal strain fields, the latter of which may be nonsymmetric.

The CP patterns taken with the beam along the y-axis appear to be composed of two four-lobe patterns, one nearly possessing four-fold symmetry and being much more intense than the

second two-fold symmetric pattern. (The reader should note that in the LS patterns shown these two patterns are hardly discernible, the distinctions being lost in the reproduction of the figures.) The more intense pattern displays a distinct maximum in intensity as a function of θ and is believed to clearly be of spherulitic origin. It is somewhat surprising that this more intense pattern is not more deformed (less four-fold symmetric) but this probably indicates that during annealing considerable relaxation and some recrystallisation of the deformed spherulite has occurred in the core – in fact a differential thermal analysis of the film core shows that two endotherms exist. This observation somewhat conflicts with the previously discussed patterns from XY and YZ sections where spherulitic deformation still seemed evident. Again, further explanation is not available to reconcile these differences; however, the complex yet unknown symmetry of the internal strain fields may well play a significant part in this discussion. In fact, the effect of strain may well be responsible for the second four-lobe patterns of weak intensity in fig. 10d. An alternative explanation for the second four-lobe pattern could be that during the deformation processes and annealing the optic axis in the spherulite is allowed to change in direction with respect to the radius of the spherulite. The degree of change in the optic axis may also be dependent on the location within the spherulite itself, i.e. polar versus an equitorial region. Such considerations have been treated theoretically by Stein *et al* [10]; an example is shown in fig. 11 where it is clear that an eight-lobe pattern can be generated under such conditions. We would speculate that all the above explanations may be important in this complex deformation process which has been followed by an annealing treatment. In summarising fig. 10, it is apparent that: (*a*) the use of XYZ light scattering is more informative than *x*-axis light scattering alone in reflecting the complex morphology that exists in such deformed materials; in fact, the existence of the three zone texture would have been completely overlooked by *x*-axis scattering alone: (*b*) the superstructure of the core material still reflects the existence of a spherulitic texture embedded in an amorphous matrix where probably both matrix plus spherulite still maintain high internal strains; (*c*) the simple model proposed of the "flattened football" like spherulite is in general agreement with the experimental data from the core material.

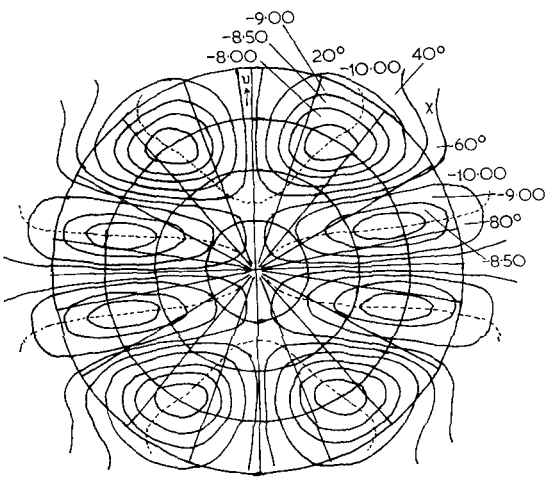

Figure 11 Theoretical *x*-axis light scattering pattern calculated for a deformed spherulite where the optic axis of the fibrils composing the spherulite is permitted to change direction with respect to the fibril axis during deformation (from Stein *et al* [10]). Stretch direction is vertical.

Discussion is now directed at the material at the edges, i.e. the edges nearest the rolled surfaces. Figs. 12a-i summarise the types of *y*-axis light scattering patterns observed in each edge as well as the core. Case II CP patterns were the more typical of those seen. From the edge patterns we note several significant points which are listed below:

(1) The core patterns of d or f are nearly superpositions of the respective edge patterns.

(2) The edge patterns reflect a single oriented superstructure with each edge being essentially the mirror image of its opposite.

(3) The shape of each pattern, e.g. b or h may well be indicating the nature of the spherulitic breakdown.

With respect to this latter point, one notes the two fold symmetry of patterns b and h. Certainly little true spherulitic structure is left since the PP patterns c or i do not show typical spherulitic scattering. Also, these patterns give evidence that the principal polarisability axis is no longer aligned with the electric vector of either the polariser or analyser. This is not surprising since the wide angle X-ray data indicate that the *c*-axis of the crystals at each edge ($\pm$ X) are tilted inward toward the core and are not well aligned along Z. Keller's data also established such evidence of crystal tilt [4]. Since the principal polarizability would be along the chain axis in

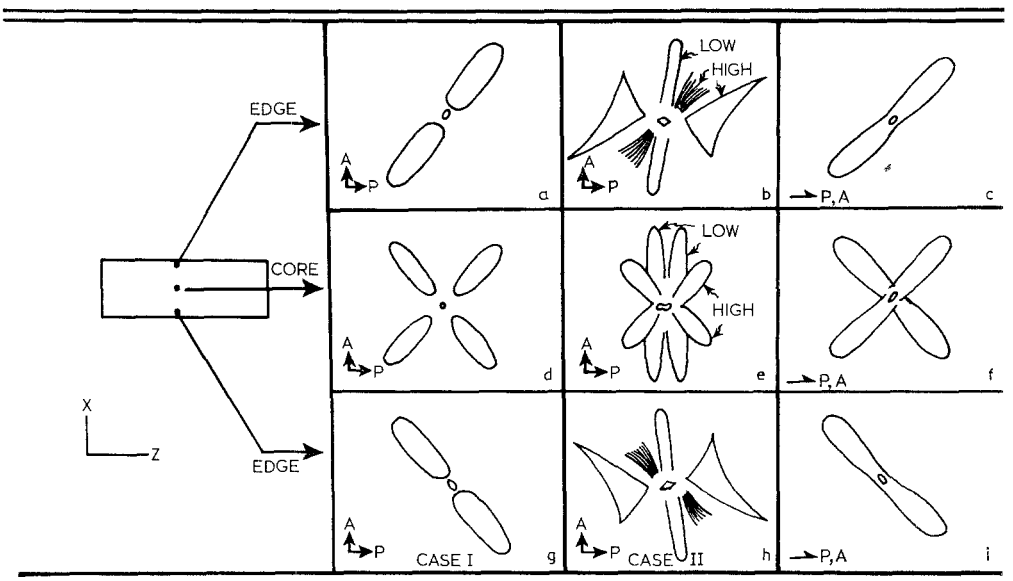

Figure 12 Sketched summary of some *y*-axis CP and PP LS patterns taken in the core and edges of the rolled and annealed film. The labels "high" and "low" refer to the degree of intensity of the indicated portions of the patterns. Compare these with fig. 9. Two sets of CP patterns are shown; Case II was the more typical.

polyethylene (*c*-axis of crystal), it is understandable that the *y*-axis edge LS patterns display this swirl-like pattern whereas the core patterns are symmetric about either the *z* or *x*-axis. These latter two axes are the major and minor axes of polarizability respectively at the core. It may well be, in fact, that near the edges, the material when rolled, undergoes an irreversible shearing deformation. With further deformation the spherulite would probably begin to undergo heterogeneous rupture due to the fact that the internal strains acting on the spherulite would be non-uniform. In fact, such rupture would be most likely to occur when the surrounding amorphous material could no longer display extensibility to absorb the energy input (work by shearing during rolling). Due to the mode of deformation it would clearly seem that the material along the maximum shear line would reach this critical limit first thereby initiating rupture of the spherulite along a similar shear plane. Further investigations are now being conducted using different degrees of rolling and annealing temperatures which will hopefully elucidate this rupture mechanism. Microscopy investigations are also being undertaken.

It seems worthwhile to comment briefly on the effect of annealing the rolled film, and at the same time to point out that the light scattering shows there are not three distinct superstructures but actually a more continuous change in texture as one goes from one rolled edge to the other. Fig. 13 shows a series of *y*-axis CP and PP patterns for both unannealed (NA) and annealed (A) films where each pattern of the series represents a different distance from a given edge as shown in the figure. A number of interesting points can be noted from these patterns:

(*a*) There is a continuous change in the shape of the CP patterns as one goes from one edge to the other. This holds for both annealed and unannealed material. This is in fact in good correspondence with Keller's [4] observation of the orientation of the lamellar normals. We were unable, however, to obtain similar results for the unannealed material using wide angle X-ray diffraction, with the beam along Y. In fact, our measurements to date show that in the unannealed films, edge and core diffraction patterns were essentially identical while for the annealed material they were not as has already been discussed – see figs. 3a and *b*. Further work is necessary to disprove or verify the above observation.

(*b*) A second significant point is that from comparison of annealed with unannealed CP patterns it is apparent that annealing at 92°C allowed relaxation to occur in the deformed

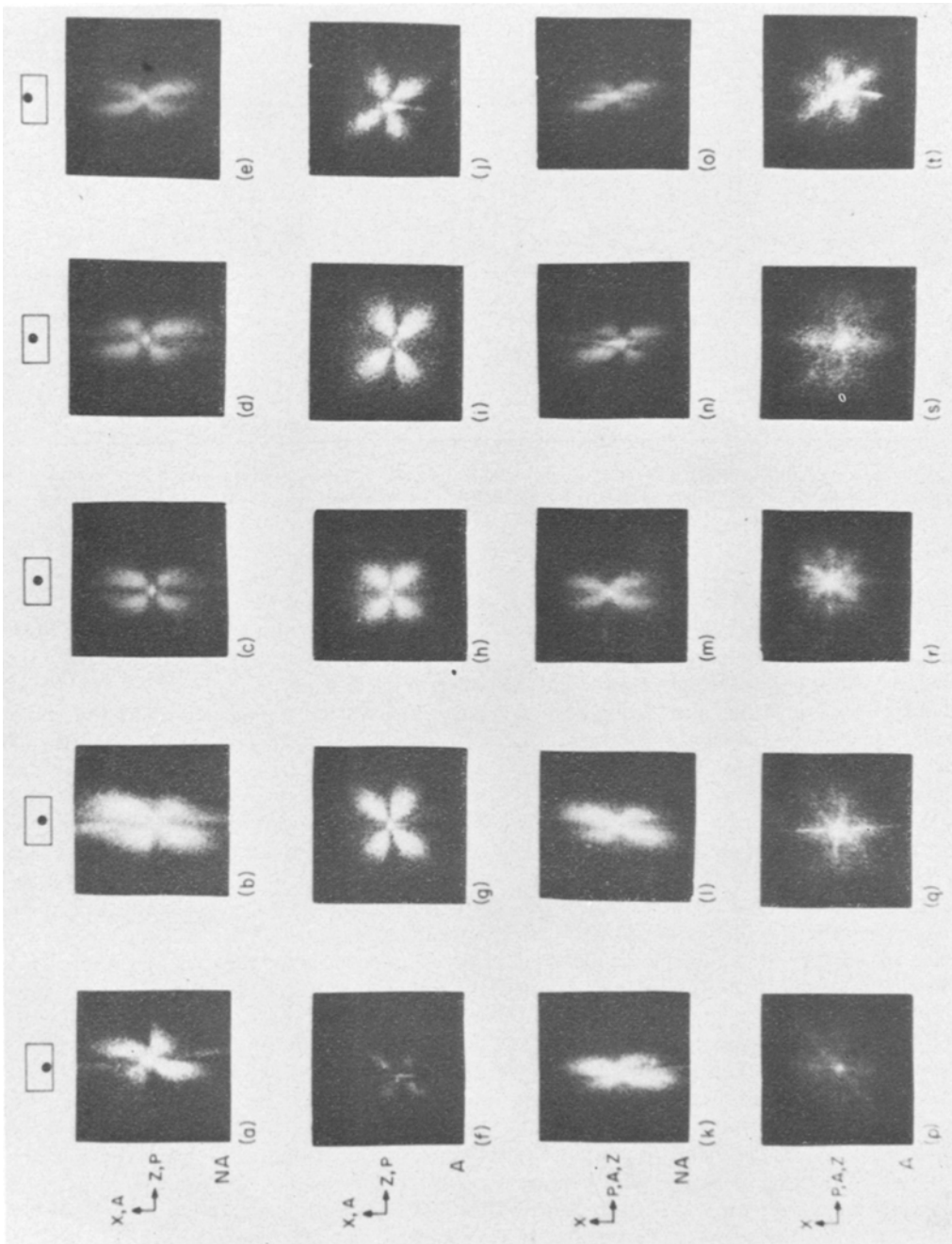

Figure 13 CP and PP *y*-axis LS patterns taken of rolled and annealed (A) and rolled and unannealed (NA) material. The boxes with the dot above each column of patterns indicate the location where the laser beam entered the sample.

superstructure. This, of course, would be expected, but it is very clearly illustrated by the fact that there is a definite trend toward increased four-fold symmetry in the annealed material. This suggests one or both of two things. First, the highly deformed unannealed spherulitic structure relaxes to a less deformed spherulite with some recrystallisation occurring, and two, there is undoubtedly a decrease in the internal strain fields which existed after rolling. This decrease in internal strain is reflected by the fact that there is indeed a more apparent maximum in the four lobes after annealing. The aspects of this have also already been discussed.

(*c*) The PP patterns of the unannealed sample are very similar to the CP patterns for the same material. This is definitely not so for the annealed film. We have no sound explanation for these differences at this time but again can only speculate that the effects of internal strains may well be of paramount importance in the explanation of these data.

To illustrate how the sample deforms during the rolling operation, a line of black ink was intentionally placed in an undeformed sample such that the dye line was parallel to the *x*-axis. The sample was then put through the roller and the profile of the dye line was found to become parabolic as is illustrated in fig. 14. The profile is of the opposite curvature of what is found for a velocity profile of fluid pipe flow. This is expected since the maximum shear gradient will be at the core whereas in pipeflow it is at the wall. The LS scattering data are clearly in correspondence with this profile in that the mirror image effect is to be expected. The result of this shear gradient results in initial spherulitic breakdown at the edges which then transcends toward the core. Whether such spherulitic breakdown will be complete throughout the sample will probably depend on such factors as rolling speed, ratio of roller gap to sample thickness, crystallinity (which affects extensibility), etc. The further effect of annealing these rolled samples is to partially relax and recrystallise a portion of the material but in a preferred manner. There is obviously still much to learn about how the final morphology depends upon thermal treatments and the other variables given above.

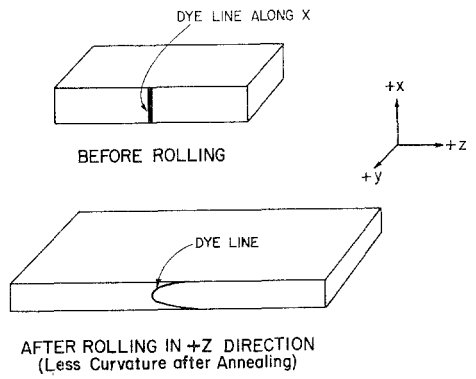

Figure 14 Drawing showing how the profile of a line of dye was affected by the rolling operation.

5. Conclusions

It is apparent that deformation by unidirectional rolling indeed results in a highly complex superstructure as shown by XYZ light scattering. Subsequent annealing as described in this work shows a complex superstructure still exists but yet appears to retain more of a spherulitic texture. The existence of true spherulitic texture is somewhat complicated by the wide angle X-ray diffraction and Keller's small angle X-ray diffraction pole figure analysis. Further studies are in order to aid in elucidating how all these data are consistent with a model – particularly for the material closest to the rolled edges. Specifically, it is suggested from the data so far that spherulitic deformation with intercrystalline reordering occurs in the core area while at the edges spherulitic rupture may well be occurring, leading toward a true single texture with extended amorphous chains having been pulled out from the spherulitic fibrils. The fact that the texture at the edges is different from the core illustrates the nonhomogeneity of the rolling process and hence suggests such rolled materials could actually be classified as a pseudo laminated material since the material at the edges would most probably exhibit different mechanical properties than that at the core. Needless to say, it can be concluded that there is still much to be learned about the effects of rolling on the morphology of polymeric materials. It is also clear that the application of XYZ light scattering can be successfully applied in illustrating the complex superstructure in biaxially oriented polyethylene. There is a definite need, however, for more theoretical scattering calculations which consider new models and which illustrate the effects of birefringence on the scattering behaviour. This latter effect is important as has been demonstrated [12-14]. Hopefully, these calculations will be

inspired and undertaken as a result of this new application of photographic light scattering.

Acknowledgement

The author would like to acknowledge the assistance of Mr A. Coe of the Textile Research Institute who so kindly carried out the electron-microscopy studies.

References

1. I. L. HAY and A. KELLER, *J. Mater. Sci.* **1** (1966) 41.
2. *Idem, ibid* **2** (1967) 538.
3. A. COWKING, J. G. RIDER, I. L. HAY, and A. KELLER, *ibid* **3** (1968) 646.
4. J. J. POINT, G. A. HOMES, D. GEZOVICH, and A. KELLER, *ibid* **4** (1969) 908.
5. R. S. STEIN and M. B. RHODES, *J. Appl. Phys.* **13** (1960) 1873.
6. R. J. SAMUELS, *J. Polymer Sci.* C, **13** (1966) 37.
7. T. INOUE, M. MORITANI, T. HASHIMOTO, and H. KAWAI, *Polymer Preprints* **11** (1970) 414.
8. M. L. WALLACH, *J. Polymer Sci.* C, **13** (1966) 69.
9. G. L. WILKES, *J. Polymer Sci.* A-2, to be published.
10. R. S. STEIN, P. ERHARDT, J. J. VAN AARTSEN, S. CLOUGH, and M. RHODES, *J. Polymer Sci.* C, **1** (1966).
11. R. S. STEIN and F. L. WILKES, *ibid* A-2, **7** (1969) 1695.
12. R. S. STEIN, P. F. ERHARDT, and W. CHU, *ibid* A-2, **7** (1969) 271.
13. D. L. LEGRAND, *ibid* A-2, **7** (1969) 279.
14. *Idem, ibid*, A-2, **11** (1970) 1937.

Received 18 November 1970 and accepted 29 June 1971.